Separation and Purification Technology 382 (2026) 136001

Contents lists available at ScienceDirect

Separation and Purification Technology

journal homepage: www.elsevier.com/locate/seppur

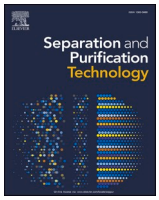

Performance assessment of different reactants in reactive-extractive distillation with unexpected discovery of new configuration

I Gede Pandega Wiratama [a,b], Zong Yang Kong [a,c,*], Ao Yang [d,*], Agus Saptoro [e,f], Basil T. Wong [a], Juan Gabriel Segovia-Hernández [g], Jaka Sunarso [a]

[a] Research Centre for Sustainable Technologies, Faculty of Engineering, Computing and Science, Swinburne University of Technology, Jalan Simpang Tiga, Kuching 93350, Sarawak, Malaysia
[b] Research Center for Renewable Energy Conversion, Faculty of Engineering Technology, Parahyangan Catholic University, Jalan Ciumbuleuit 94, Bandung 40141, West Java, Indonesia
[c] School of Engineering, Faculty of Engineering and Technology, Sunway University, No. 5, Jalan Universiti, Bandar Sunway, 47500, Selangor Darul Ehsan, Malaysia
[d] College of Safety Science and Engineering, Chongqing University of Science & Technology, Chongqing 401331, PR China
[e] Western Australian School of Mines, Curtin University, Locked Bag 30, Kalgoorlie, WA 6433, Australia
[f] Curtin Malaysia Research Institute, Curtin University Malaysia, CDT 250, Miri 98009, Sarawak, Malaysia
[g] Universidad de Guanajuato, Campus Guanajuato, División de Ciencias Naturales y Exactas, Departamento de Ingeniería Química, Noria Alta s/n, 36050 Guanajuato, Gto, Mexico

ARTICLE INFO

Editor: Cintia Marangoni

Keywords:
Azeotropic separation
Hydration reaction
Sustainability
Process intensification
Multi-objective optimization

ABSTRACT

Reactive-extractive distillation (RED) has been widely studied for separating water-containing ternary azeotropes, particularly since 2020. However, most existing studies have employed ethylene oxide (EO) as the reactive agent, leaving the potential of alternative reactants largely unexplored. This study addresses this gap by directly comparing double-column RED (DCRED) systems using glycidol (GD) and EO for the separation of tetrahydrofuran (THF)/methanol (MeOH)/water mixtures as a case study. In addition, it was unexpectedly found that high-purity THF and MeOH can be recovered using only a single RED column. This discovery leads to the development of a new single-column RED (SCRED), which potentially offers a lower total capital cost compared to the conventional DCRED configuration. Three process schemes were simulated and optimized in Aspen Plus using a multi-objective genetic algorithm (MOGA), with total net revenue (TNR), CO_2 emissions, and exergy efficiency as the objective functions. Besides, total reboiler duty was included in the evaluation to provide a more comprehensive 4E assessment (economic, energy, environmental, and exergy efficiency). The comparison reveals that substituting EO with GD results in improved 4E performances. Although the increase in exergy efficiency is modest (1.2 %), DCRED with GD demonstrates significant performance enhancements compared to DCRED with EO in other aspects. It achieves 38.8 % and 38.5 % reductions in total reboiler duty and CO_2 emissions, respectively, along with a 52 % increase in TNR. Moreover, even though SCRED underperforms compared to DCRED with GD, it still offers notable advantages over DCRED with EO, delivering 50.3 % higher TNR, 19.5 % lower reboiler duty, 21.7 % lower CO_2 emissions, and 1.17 % higher exergy efficiency. Overall, the above findings demonstrate that GD is a promising and more sustainable alternative to EO in RED-based separation of THF/MeOH/water mixtures.

1. Introduction

The separation of water-containing ternary azeotropic mixtures remains a significant challenge in designing efficient and sustainable chemical processes. A conventional method to separate such mixtures is extractive distillation (ED), which typically relies on external entrainers and is highly energy intensive. To address these limitations, reactive-extractive distillation (RED) has been proposed as a more efficient alternative. RED is a hybrid process that combines the benefits of reactive distillation (RD) and ED in a single unit. The reaction is typically exothermic, reducing the reboiler duty, while the presence of a entrainer modifies relative volatilities, enhancing the separation of azeotropic mixture. Ethylene oxide (EO) is the most commonly studied

* Corresponding authors.
E-mail addresses: savierk@sunway.edu.my (Z.Y. Kong), aoyang2021@cqust.edu.cn (A. Yang).

https://doi.org/10.1016/j.seppur.2025.136001
Received 15 September 2025; Received in revised form 29 October 2025; Accepted 6 November 2025
Available online 7 November 2025

Nomenclature

4E	Economic, energy, environmental, exergy efficiency
C%	Carbon content of the fuel
C_{GD}	Glycidol concentration (M)
DCRED	Double-column reactive-extractive distillation
$e_{chem,i}$	Compound exergy of component "i"
ED	Extractive distillation
EG	Ethylene glycol
EO	Ethylene oxide
ERC	Entrainer recovery column
Ex_D	Exergy destruction
Ex_{in}	Exergy input
Ex_{out}	Exergy output
GD	Glycidol
GR	Glycerol
H	Stream enthalpy flow (kW)
HPS	High pressure steam
h_{seq}	Steam enthalpy (kJ kg^{-1})
ID	Inside diameter (m)
LPS	Low pressure steam
MeOH	Methanol
MOGA	Multi-objective genetic algorithm
MPS	Medium pressure steam
NHV	Net heating value (kJ kg^{-1})
N_T	Total stages number for each column
N_E	Entrainer stage location
N_F	Feed stage location
N_R	Reactant stage location
N_{SS}	Side-stream stage
Q_{fuel}	Energy consumption of the process (kJ h^{-1})
Q_R	Reboiler duty (kJ h^{-1})
r	Reaction rate (kmol m^{-3} s^{-1})
RED	Reactive-extractive distillation
REDC	Reactive-extractive distillation column
RR	Reflux ratio
S	Stream entropy flow (kW K^{-1})
SA	Sulfuric acid
SCRED	Single-column reactive-extractive distillation
T_0	Ambient temperature (K)
TAC	Total annual cost ($ per year)
T_F	Flame temperature (K)
THF	Tetrahydrofuran
TNR	Total net revenue ($ per year)
T_S	Chimney temperature (K)
$V_{hold-up}$	Liquid volume hold-up (m^3)
VLE	Vapor-liquid equilibrium
w	Weir height (m)
x_{EO}	Mole fraction of EO
x_i	Mole fraction of component "i"
x_{Water}	Mole fraction of water
α	Mole ratio of CO_2 and C
ΔH_{VL}	Enthalpy of vaporization (kJ $kmol^{-1}$)
λ	Latent heat of steam (kJ kg^{-1})
η	Exergy efficiency

reactive agent, often referred to as "the reactant". EO reacts with water to form ethylene glycol (EG), effectively removing water from the mixture. EG also acts as an entrainer, enhancing relative volatilities and breaking azeotropes. This concept was first introduced by Su et al. [1], who applied RED to separate a Tetrahydrofuran (THF)/Ethanol (EtOH)/water mixture. They reported that a triple-column RED (TCRED) reduced total annual cost (TAC) by 63 % and CO_2 emissions by 84 %, compared to pressure swing distillation (PSD). Following this, many other researchers reported the superiority of RED over conventional methods in separating water-containing ternary mixtures. For instance, Wang et al. [2] showed that, for the separation of ethyl acetate (EtAc)/EtOH/water, TCRED reduced TAC by up to 32 % compared to triple-column ED (TCED). In another example, Wang et al. [3] demonstrated that, for THF/methanol (MeOH)/water separation, double-column RED (DCRED) could reduce TAC by up to 38 % compared to TCED. Several intensified RED configurations have also been investigated. Liu et al. [4] reported that a dividing-wall RED (DW-RED) coupled with an organic Rankine cycle could save up to 27.5 % in TAC compared to DCRED. Kong et al. [5] introduced side-stream RED (SS-RED), which achieved reductions of 21 % in TAC, 29 % in CO_2 emissions, 19 % in inherent safety risks, and 97 % in the condition number relative to DCRED.

Until here, it is important to note that studies on RED for water-containing ternary azeotropic mixtures conducted up to 2024 have consistently used EO as the reactant, as shown in Table 1. While EO is frequently employed in RED research, its high flammability poses a major barrier for its scaling up and industrial deployments. Consequently, the search for a less flammable, highly effective, alternative reactant becomes imperative to address the safety concerns [6]. In 2025, Wiratama et al. [7] proposed glycidol (GD) as a safer alternative. GD reacts with water to form glycerol (GR), which can also act as an entrainer, specifically for THF/MeOH/water mixture. Compared to EO, GD has a significantly higher flash point, up to 92 K, indicating lower flammability [8–10]. Using GD in a DCRED system for THF/MeOH/water separation was reported to reduce TAC by 25.3 % compared to TCED [7]. Therefore, RED systems using GD show promising economic performance compared to conventional ED. However, a critical knowledge gap remains as there is no direct comparison between RED systems using EO and those using GD [11]. This study addresses that gap by providing a detailed comparative analysis where to date such a comparative study has not yet been reported. Comparing RED with EO and RED with GD is essential, as the benefit of GD in terms of flammability must be weighed against its overall process performance. Thus, originally this work focused on two configurations, which are DCRED with EO (Case 1) and DCRED with GD (Case 2). However, upon exploring ways to intensify Case 2, a surprising finding led to the development of a third option, i.e., a single-column RED (SCRED), referred to as Case 3. Unlike the conventional DCRED, which requires both an RED column (REDC) and an entrainer recovery column (ERC), the SCRED configuration utilizes only a single REDC with a side-draw stream. With this design, high-purity ($\geq$ 0.995 mole fraction) THF and MeOH can be simultaneously recovered from the distillate and side-draw streams, respectively. Furthermore, the entrainer is directly recovered from the bottom product of the same column, eliminating the need for a second column for entrainer recovery. To the best of our knowledge, this type of configuration has not been reported in previous studies, adding a novel contribution to this work. The finding that triggered this development, along with a detailed explanation of how SCRED was designed, is discussed in Section 3.2.

To conduct a comprehensive analysis, the comparison between all cases includes not only the economic aspect but also the energy, environmental, and exergy efficiency aspects, collectively referred to as the 4E framework. As reported by Sholl and Lively [39], chemical separations account for approximately half of industrial energy consumption. Of this, about 80 % is used in thermal separation processes, including 49 % for distillation, 20 % for drying, and 11 % for evaporation. Given the dominant role of distillation-based processes in overall plant energy use, evaluating the energy performance of the systems is essential. Moreover, energy consumption is closely linked to environmental impact, as higher

Table 1
Summary of RED research for separating water-containing ternary azeotropic mixture (up to August 5, 2025).

Year	References	Mixture	Reactant	Comparison	Assessment
2020	Su et al. [1]	THF/EtOH/water	EO	TCRED to PSD	Economic and environmental
2021	Wang et al. [2]	EtAc/EtOH/water	EO	DCRED to TCRED	Economic
	Li et al. [12]	Acetonitrile (ACN)/isopropanol (IpOH)/ water	EO	TCRED to TCRED with heat integration (HI)	Economic, energy, environmental, exergy
	Zhang et al. [13]	Tert-butanol (TBA)/EtOH/water, THF/ EtOH/water, ACN/IpOH/water	EO	DCRED to DCRED with feed-effluent heat exchangers (FEHE)	Economic
2022	Liu et al. [4]	EtAc/EtOH/water	EO	DW-RED to DCRED	Economic, safety, environmental
	Kong et al. [5]	THF/EtOH/water	EO	SS-RED to DCRED	Economic, safety, environmental, controllability
	Kong et al. [14]	Diisopropyl ether (DIPE)/IpOH/water	EO	DCRED with pre-concentration column (PC) to conventional ED	Economic, energy, environmental, exergy efficiency
	Wu and Chien [15]	THF/EtOH/water, TBA/EtOH/water	EO	Various control strategy on DCRED	Control performance
	Wu et al. [16]	Cyclohexane/IpOH/water	EO	Various water composition in the feed stream	Economic
	Yan et al. [17]	Benzene/IpOH/water	EO	DW-RED to DCRED	Economic, environmental, exergy
	Yang et al. [18]	TBA/EtOH/water	EO	DW-RED to DCRED	Economic, environmental, exergy efficiency
2023	Du et al. [19]	THF/MeOH/water	EO	DW-RED to DCRED	Economic, safety, environmental
	Huang et al. [20]	IpOH/EtAc/water	EO	DW-RED to DCRED	Economic, environmental, exergy
	Kong et al. [21]	ACN/IpOH/water	EO	DCRED with and without side reaction	Economic
	Liu et al. [22]	EtAc/EtOH/water	EO	Various control strategy on DW-RED	Control performance
	Yang et al. [23]	IpOH/EtAc/water	EO	SS-RED to DW-RED	Economic, energy, environmental, exergy efficiency
2024	Wang et al. [3]	THF/MeOH/water	EO	DW-RED to DCRED	Economic, energy, environmental, exergy
	Chen et al. [24]	THF/EtOH/water	EO	ED-RD to DCRED	Economic
	Huang et al. [25]	IpOH/EtAc/water	EO	Various control strategy on DCRED	Control performance
	Neyestani and Eslamloueyan [26]	THF/MeOH/water	EO	TCRED to TCED	Economic, environmental
	Qi et al. [27]	Dioxane (DIO)/EtAc/water	EO	Various water composition in the feed stream	Economic, environmental, exergy efficiency
	Rui et al. [28]	EtOH/DIO/water	EO	SS-RED with intermediate reboiler to DCRED	Economic, entropy
	Sánchez-Ramírez et al. [29]	EtAc/EtOH/water	EO	Reaction stages	Economic
	Teh et al. [30]	THF/EtOH/water, EtAc/EtOH/water	EO	TCRED with and without side reaction	Economic, energy, environmental
	Teh et al. [31]	ACN/IpOH/water, EtAc/EtOH/water, EtAc/ IpOH/water	EO	DCRED with process-to-process heat exchanger to DCRED	Economic
	Yin et al. [32]	DIPE/IpOH/water	EO	DW-RED to DCRED	Economic, energy, environmental, exergy
	Zhang et al. [33]	THF/MeOH/water	EO	TCRED with HI to TCED	Economic, energy
2025	Kong et al. [34]	ACN/IpOH/water	EO	Side-stream thermally-coupled RED (ST-RED) to DCRED	Economic, energy
	Liu et al. [35]	TBA/EtOH/water	EO	Optimization framework	Economic
	Wiratama et al. [7]	**THF/MeOH/water**	**GD**	**DCRED to TCED**	**Economic, safety**
	Zhu et al. [36]	TBA/EtOH/water	EO	DCRED with HI to DCRED	Economic, energy, environmental, exergy
	Zou et al. [37]	Toluene/n-butanol/water	EO	DCRED to PSD with decantation	Economic, environmental, exergy efficiency
	Jin et al. [38]	THF/MeOH/water	EO	DW-RED to DCRED	Economic, environmental, safety
	This work	**THF/MeOH/water**	**GD, EO**	**DCRED with EO, DCRED with GD, and SCRED**	**Economic, energy, environmental, exergy**

energy usage typically results in increased greenhouse gas emissions, particularly CO_2, a major contributor to global warming. According to the Paris Agreement, global temperature rise should be limited to within 2 °C this century, with a preferred target of 1.5 °C compared to pre-industrial levels [40]. One of the key strategies to meet this target is reducing CO_2 emissions from industrial processes. Therefore, assessing the CO_2 emissions of each process is integral to aligning with global climate goals. Additionally, exergy analysis offers a meaningful measure of how efficiently energy is utilized within the system. Through this 4E evaluation, the sustainability and overall performance of each RED configuration can be comprehensively assessed.

For a fair comparison, it is essential to optimize each process to ensure that performance metrics are based on the best design and operating conditions. However, single-objective optimization is insufficient to handle trade-offs among multiple performance aspects in the 4E framework. Traditional methods, such as sensitivity analysis or sequential iterative optimization, often get trapped in local optima and fail to identify the global optimum. Therefore, global multi-objective optimization methods are more appropriate. Given the complexity and strong nonlinearity of separation process modeling, stochastic optimization algorithms such as genetic algorithms (GA) have proven effective [41]. Several RED studies have successfully applied GA for process optimization. For example, Wang et al. [2] used GA to optimize a RED system for separating an EtOH/EtAc/water mixture using TAC as the objective function. Zhao et al. [42] employed a multi-objective GA (MOGA) to simultaneously minimize TAC and gas emissions. Yan et al. [17] extended the implementation of MOGA by optimizing three objectives, i.e., TAC, CO_2 emissions, and exergy efficiency. Based on these examples, MOGA has shown strong applicability to RED systems. Accordingly, in this work, all processes were optimized using MOGA with objective functions of total net revenue (TNR), CO_2 emissions, and exergy efficiency. In addition, to provide a more comprehensive 4E assessment, the total reboiler duty was included in the evaluation stage.

In summary, this study aims to present the first direct comparison between DCRED processes using EO and GD for the separation of MeOH/THF/water under optimized conditions. In addition, a newly developed

SCRED configuration, which emerged from a surprising finding, is included for comparison. By integrating MOGA optimization with a 4E evaluation framework, this work provides a balanced and comprehensive assessment of both economic performance and sustainability. The findings are expected to guide the selection of more effective reactant for RED applications and to offer valuable insights into intensified separation technologies.

2. Methodology and design basis

This work uses the separation of a THF/MeOH/water mixture as a case study since this system was also studied previously in the first application of GD in a RED process [7]. Such mixtures are commonly encountered in various industries, including polyvinyl chloride production, magnetic film manufacturing, and the synthesis of 1,4-butanediol *via* maleic anhydride esterification [26,43]. The scope of this study is limited to process simulation. Aspen Plus was used to develop the process flowsheet, which was then integrated with MATLAB *via* Component Object Model (COM) for optimization purposes. The overall framework of the study is presented in Fig. 1.

In Aspen Plus, the Non-Random Two Liquid model with the Redlich-Kwong equation of state (NRTL-RK) was selected as the thermodynamic package. This hybrid model applies the NRTL equation for the liquid phase and the Redlich-Kwong (RK) equation for the vapor phase. Any missing binary interaction parameters were estimated using the UNIFAC method. The NRTL model has been widely applied in systems involving THF/MeOH/water [44–46]. Several studies have also shown that vapor-liquid equilibrium (VLE) predictions using NRTL-RK closely match experimental data [47–49]. For example, Danov et al. [49] compared the performance of the NRTL and UNIQUAC models for a system containing GD, MeOH, GR, and water. Consistent with our approach, they estimated missing binary interaction parameters using UNIFAC and found that the NRTL model provided a better fit to experimental VLE data than the UNIQUAC model. Additionally, they reported that the RK equation of state offered a more accurate representation of the vapor phase than the ideal gas model. Based on this literature review, we conclude that the NRTL-RK model is a reliable and suitable choice for our simulation study. The binary interaction parameter values are summarized in Table S1 of the Supporting Information.

2.1. Reaction kinetic

The reaction kinetics for the water-EO system are shown in Eq. 1. This kinetic expression, originally derived from Huang et al. [50], has been widely adopted in RED research [23,32,51]. In contrast, the reaction kinetics for the water-GD system are shown in Eq. 2, based on the work of Vermeulen et al. [52]. This kinetic model has been applied in RED simulations by Wiratama et al. [7]. It is essential to note that the water-EO reaction in Eq. 1 represents an uncatalyzed reaction [50], whereas the water-GD reaction in Eq. 2 was derived from experiments using sulfuric acid (SA) as a catalyst, at a concentration of 0.075 mol kg^{-1} [52].

$$EO + Water \rightarrow EG \tag{1}$$

$$r\left(kmol\ m^{-3}s^{-1}\right) = 3.15 \times 10^{12} exp\left(-\frac{9547}{T}\right) x_{Water}\ x_{EO}$$

where r represents reaction rate; x_{Water} and x_{EO} represent mole fraction of water and EO, respectively; T represents temperature in K.

$$GD + Water \rightarrow GR \tag{2}$$

$$r\left(kmol\ m^{-3}s^{-1}\right) = 1.275 \times 10^{10} exp\left(-\frac{8827}{T}\right) C_{GD}$$

with C_{GD} represents molar concentration of GD (kmol m^{-3}). It is critical to point out that the kinetics of the EO-water reaction has been extensively exploited in most RED studies, indicating its reliability. Moreover, the applicability of the GD-water reaction kinetics has been discussed and validated in a previous study [7]. In summary, the kinetics were applied in simulations of both the reactor-distillation sequence and the RD systems. The experimental results were well reproduced by the simulations, and the percentage error remained within the experimental uncertainty range reported in the literature. However, reiterating the same detailed discussion in the present manuscript would be redundant and reduce conciseness. Therefore, readers interested in a more detailed explanation are kindly referred to our previous work [7].

2.2. Basic flowsheet

The process flowsheet for Case 1 is shown in Fig. 2, representing a DCRED system. A mixture of THF/MeOH/water enters the REDC at a flow rate of 100 kmol h^{-1}, a pressure of 1 atm, and a temperature of 335 K. The mole fractions of THF, MeOH, and water in the feed stream are 0.408, 0.392, and 0.2, respectively. These values were directly adopted from the previous study [7]. In addition to the feed stream, two other streams are introduced into the REDC, which are the reactant stream (F_R) and the entrainer stream (F_E). F_E is a recycled stream originating from the bottom of the second column, i.e., the ERC. In contrast, F_R is a fresh input stream containing 20 kmol h^{-1} of EO, maintaining a 1:1 mole ratio with water to satisfy the reaction stoichiometry. In the REDC, EO reacts with water to produce EG. Since the reaction is homogeneous, it occurs on all stages of the column [53]. The liquid hold-up per tray is calculated using Eq. 3, while the hold-up in the reflux drum and reboiler sump is assumed to be ten times that of a single tray [54].

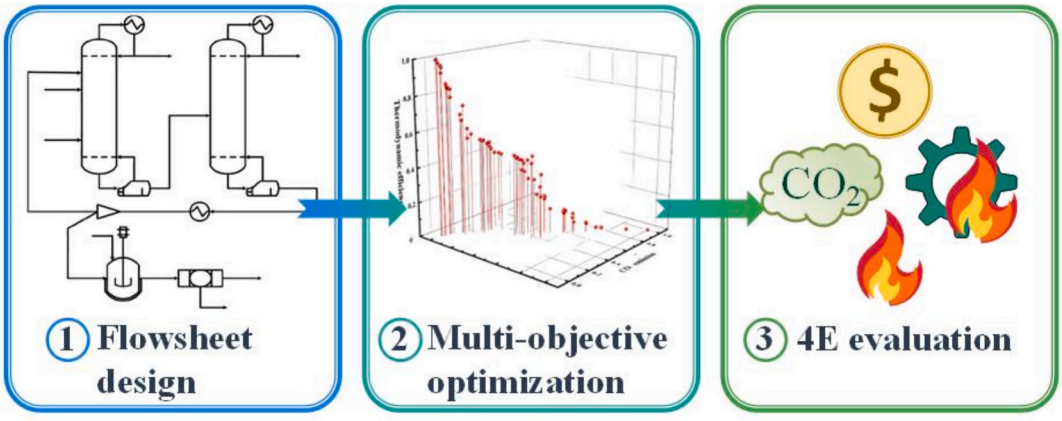

Fig. 1. The framework of this study.

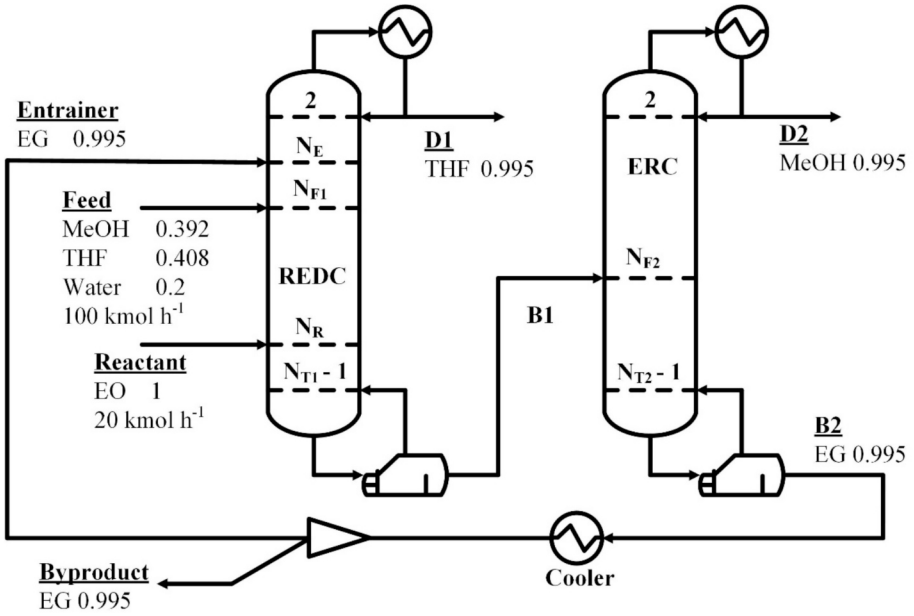

Fig. 2. Basic flowsheet of Case 1 (DCR ED with EO). All compositions are in mole fraction.

$$V_{hold-up} = 0.9 \times \frac{1}{4} \times \pi \times w \times ID^2 \quad (3)$$

where $V_{hold\text{-}up}$ represents the liquid hold-up volume (m^3); w represents weir height (m); and ID represent column inside diameter (m).

The reaction product, EG, acts as an entrainer, breaking the azeotrope between THF and MeOH. As a result, THF is recovered as the distillate, while EG and MeOH exit as the bottom stream and are sent to the ERC. In ERC, MeOH is separated from EG. MeOH is recovered as the distillate, while EG is discharged as the bottom stream. A portion of this bottom stream is recycled back to REDC as F_E, since it primarily contains the entrainer (i.e., EG). The remaining portion must be withdrawn from the system to avoid accumulation, as EG is continuously produced from the EO-water reaction.

The process flowsheet for Case 2 is illustrated in Fig. 3, which also represents a DCRED system, but with the addition of a neutralization section. In this case, the F_R stream contains 20 kmol h^{-1} of GD, again maintaining a 1:1 mole ratio with water to satisfy the reaction stoichiometry. A small amount of SA is added as a make-up catalyst (included in the F_R). The required SA mole flow rate is calculated using the

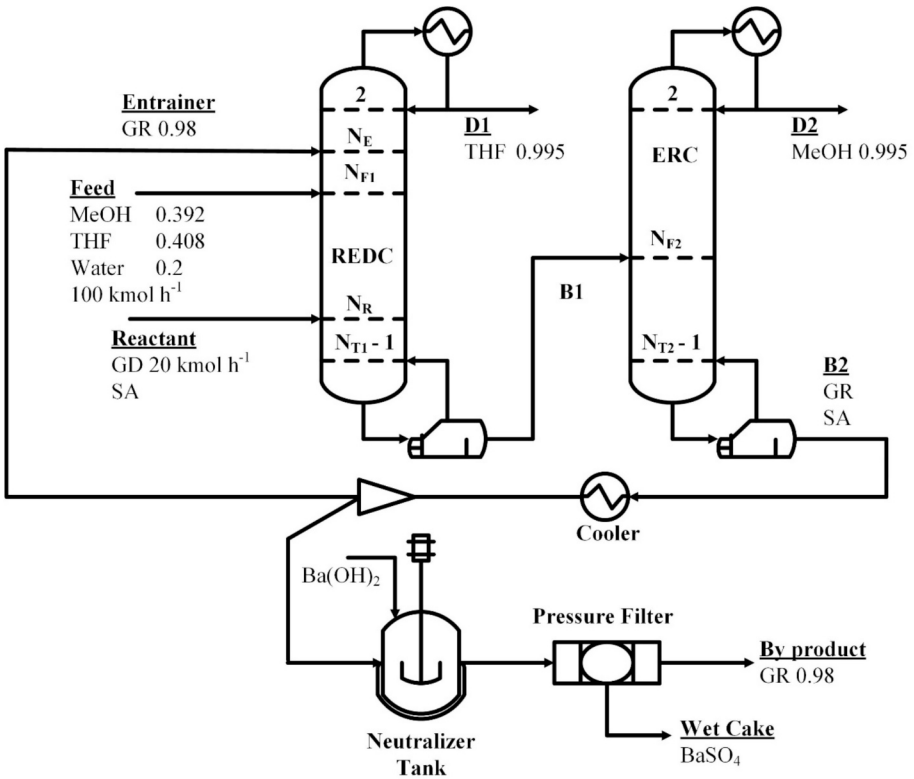

Fig. 3. Basic flowshe et of Case 2 (DCRED with GD). All compositions are in mole fraction.

Calculator Tool in Aspen Plus to ensure a concentration of 0.075 mol kg^{-1}, in accordance with literature data [52]. This SA concentration is defined per kilogram of the total stream entering the REDC, which consists of the feed stream, F_R, and F_E. Accordingly, a Calculator block is used to determine the required amount of SA make-up in the F_R, taking into account that a portion of SA is already present in the F_E. The calculated value may vary during the optimization, with the final results presented in Section 3 (Figs. 7 and 11).

Since GD is used as the reactant in this case, the reaction produces GR, which functions as the entrainer. A portion of the GR stream is recycled to REDC, while the remainder must be purged to prevent accumulation. Unlike Case 1, which operates without a catalyst, this configuration involves SA, which exits the system along with the purged GR stream. Commercial listings on Ref. [55] show that GR with a mole fraction of 0.95 is still considered marketable, with water being its primary impurity. However, in this case, the purged GR also contains residual SA, which must be removed before the product can be sold. Therefore, purification is required to meet market standards. For this purpose, a neutralization tank and filtration unit are added downstream of the DCRED system. These units are modeled in Aspen Plus using the REquil and Filter modules. Since the acid-base reaction rate is extremely fast, often occurring on the microsecond scale [56], a residence time of 1 min in the neutralization tank was assumed to be sufficient. In the neutralization tank, barium hydroxide ($Ba(OH)_2$) is added to react with SA, forming an insoluble salt ($BaSO_4$) and water, as shown in Eq. 4. The resulting $BaSO_4$ is removed using a pressure filter. The wet cake produced by the filter has a residual moisture content of 0.33 (mass fraction) [57]. To achieve this target moisture content, the Design Spec tool in Aspen Plus was employed, with the liquid-to-liquid split fraction in the filter unit used as the manipulated variable. The filtrate leaving the filter is a GR-rich by-product stream with a mole fraction of 0.98, in which water (formed by the neutralization reaction) is the main impurity.

$$H_2SO_4 + Ba(OH)_2 \rightarrow BaSO_4 + 2\,\text{Water} \quad (4)$$

The flowsheet for Case 3 consists only of the REDC and neutralization sections, as shown in Fig. 4. In this case, three streams are drawn from the REDC, i.e., the distillate stream, the side stream, and the bottom stream. THF is recovered in the distillate stream, MeOH in the side stream, and GR in the bottom stream. Similar to Case 2, the GR stream is split, with one portion recycled back into the REDC and the other sent to the neutralization section. The more detailed explanation on how this configuration could work properly is discussed in Section 3.2. It is also worth noting that to maintain consistency with the previous study, zero pressure drop were assumed for all cases [7].

2.3. Process evaluation

Case 1, Case 2, and Case 3 were evaluated based on economic, environmental, and exergy efficiency. For the economic aspect, TNR was used as it provides a comprehensive evaluation of the chemical production process. TNR reflects the profitability of producing a unit of product over a complete production cycle and accounts for the cost of raw materials, product selling prices, and TAC. The formula for TNR is shown in Eq. 5, while the detailed TAC formula was adopted from the literature [58,59] and is presented in Table S2 of the Supporting Information. TAC consists of both operating and capital costs. The calculation assumes 8000 h of operation per year and a payback period of 3 years [54]. The prices of each compound were sourced from online references [55, 60], with specific values provided in Table S3 of the Supporting Information. The cost of the fresh feed (i.e., the THF/MeOH/water mixture) was not included in the TNR calculation since it is assumed to

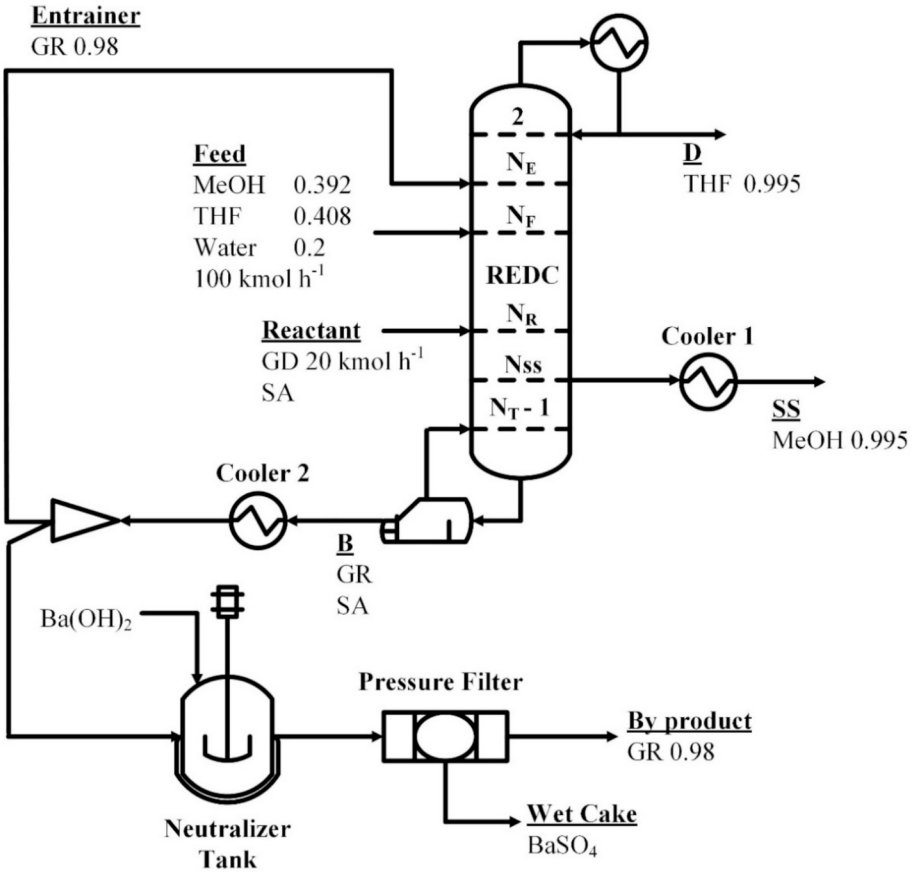

Fig. 4. Basic flowsheet of Cas e 3 (SCRED with GD). All compositions are in mole fraction.

be a waste stream or effluent from another process. In addition, the purchasing costs of SA and $Ba(OH)_2$, as well as the disposal cost of $BaSO_4$, were not included because their mass flow rates are very small compared to those of the main reactant and products.

$$\text{TNR (\$ per year)} = \sum \left(\text{value}_{\text{products}} - \text{cost}_{\text{raw materials}}\right) - \text{TAC} \quad (5)$$

In evaluating the chemical separation process, environmental assessment is based on established indicators and standards that account for the potential impact of the process on the environment. These indicators are developed in line with the principles and objectives of environmental protection, with the goal of assessing and monitoring environmental impacts to promote sustainable and responsible development. In this study, CO_2 emissions were selected as the key indicator to reflect environmental impact. As a major greenhouse gas, CO_2 contributes to global climate change, disrupts ecological balance, and poses other environmental risks. Therefore, quantifying CO_2 emissions is essential for evaluating environmental performance [61]. The specific calculation method for CO_2 emissions is provided in Eq. 6.

$$CO_2 \text{ emissions} = \frac{Q_{\text{fuel}}}{\text{NHV}} \times \frac{C\%}{100} \times \alpha \quad (6)$$

where Q_{fuel} (kJ h^{-1}) is the energy requirement from the fuel, which is calculated by Eq. 7; the net heating value (NHV) and carbon content (C %) of the fuel are 39,771 kJ kg^{-1} and 86.5, respectively; α represents the mole ratio of CO_2 and C with value of 3.67 [1].

$$Q_{\text{fuel}} = \frac{Q_R}{\lambda_{\text{seq}}} \times \left(h_{\text{seq}} - 419\right) \times \frac{(T_F - T_0)}{(T_F - T_S)} \quad (7)$$

where λ_{seq} and h_{seq} represent the latent heat and enthalpy of the steam, respectively, in the unit of kJ kg^{-1}. Q_R (kJ h^{-1}) refers to the reboiler energy consumption of the process. The flame temperature (T_F) is 2073 K, the chimney temperature (T_S) is 433 K, and the ambient temperature (T_0) is 298 K [1].

Exergy efficiency was further evaluated through exergy analysis, which assesses the effectiveness of chemical and thermal energy utilization within the separation process. Chemical energy refers to the energy involved in molecular interactions during separation, while thermal energy pertains to heating and cooling operations. Exergy analysis allows identification of energy losses and provides insight into their causes. This enables the implementation of corrective measures to reduce energy consumption. The results from the exergy analysis serves as valuable references for process design and optimization, offering a scientific basis for improving process efficiency, lowering production costs, and minimizing environmental impact. The formula used to calculate exergy efficiency is provided in Eq. 8 [42,62].

$$\eta = 1 - \frac{\text{Ex}_D}{|\sum \text{Ex}_{\text{in}}|} \times 100\% \quad (8)$$

$$\text{Ex}_D = \sum \text{Ex}_{\text{in}} - \sum \text{Ex}_{\text{out}}$$

where η represents exergy efficiency; Ex is the exergy (in kW), calculated using Eq. 9. The subscripts "in" and "out" refer to the exergy of the input and output streams, respectively. The difference between the input and output exergy is referred to as exergy destruction, denoted by Ex_D.

$$\text{Ex} = \sum (H - T_0 S) + \sum x_i \times e_{\text{chem,i}} \quad (9)$$

where H (kW) represents the enthalpy flow; S (kW K^{-1}) represents the entropy flow; x_i represents mole fraction of component "i"; $e_{\text{chem,i}}$ represents chemical exergy of the component "i". The values of chemical exergy for all components involved in this work are derived from Szargut [63] and presented in Table S4 of the Supporting Information.

2.4. Process optimization

The optimization was done by MOGA with three objective functions, which are TNR, CO_2 emissions, and exergy efficiency. Among these, TNR and exergy efficiency are maximized, while CO_2 emissions are minimized. The mathematical formulation of this multi-objective optimization is expressed in Eq. 10.

$$\begin{aligned} &\text{Maximize} && f_1(\nu_1, \nu_2, \nu_3, \ldots) = \text{TNR} \\ &\text{Minimize} && f_2(\nu_1, \nu_2, \nu_3, \ldots) = CO_2 \text{ emissions} \\ &\text{Maximize} && f_3(\nu_1, \nu_2, \nu_3, \ldots) = \eta \\ &\text{Subject to} && x_{\text{product}} \geq x_{\text{desired}} \end{aligned} \quad (10)$$

where ν_1, ν_2, ν_3, and so on represent the decision variables, which include the total number of stages, feed stage locations, side stream stage location (specific to Case 3), column pressure, and entrainer flow rate. Detailed information on the decision variables for each flowsheet, along with their boundary values, is provided in Tables S5, S6, and S7 in the Supporting Information. The term x_{product} refers to the mole fraction of the product, while x_{desired} represents the target mole fraction, which is set to 0.995, consistent with values used in the previous study. The result of the MOGA optimization is a set of optimal solutions, known as the Pareto front. Since the objective values vary significantly, for example, TNR can reach values up to 10^7, while efficiency ranges only from 0 to 1, all objective values in the Pareto front are normalized to a 0–1 scale. The normalization formula is provided in Eq. S1 of the Supporting Information. The best or most balanced solution is then selected based on the shortest Euclidean distance to the ideal point across all objectives. In this context, the ideal point is defined as having normalized TNR and exergy efficiency equal to 1, and normalized CO_2 emissions equal to 0. The formula of the shortest Euclidean distance is provided in Eq. S2 of the Supporting Information.

MATLAB and Aspen Plus were integrated using COM technology to perform the optimization with MOGA, as illustrated in Fig. 5. The optimization process terminates when one of the following stopping criteria is met: (i) the maximum number of generations is reached, (ii) the algorithm reaches the maximum number of stall generations, or (iii) the change in the spread of Pareto solutions falls below the function tolerance. In this study, default values in MATLAB were used for stopping criteria and MOGA parameters, including population size, crossover fraction, Pareto fraction, and constraint tolerance. The maximum number of generations was set to 200 times the number of decision variables, with a maximum stall generation of 100 and a function tolerance of 1×10^{-6}. The population size, crossover fraction, Pareto fraction, and constraint tolerance were set to 200, 0.8, 0.35, and 1×10^{-3}, respectively. It is important to note that optimization in this study was used solely as a tool to enhance process performance [64,65]. Additionally, to ensure a fair comparison across the three cases, all were optimized using the same method and evaluated at their respective optimal designs. As such, the effect of MOGA parameters on the optimization outcomes was not investigated, and the use of MATLAB's default values was considered sufficient. This approach is also commonly adopted in the literature on RED optimization [2,66].

3. Results and discussion

3.1. Case 1 and case 2 comparison

As mentioned in Section 1, only Case 1 and Case 2 were initially investigated. The optimized flowsheets for Case 1 and Case 2 are shown in Fig. 6 and Fig. 7, respectively. In both cases, the optimization process terminated because the change in the spread of Pareto solutions fell below the specified function tolerance. The final Pareto fronts for Case 1 is shown in Fig. 8, while for the other cases are shown in Fig. S1 and

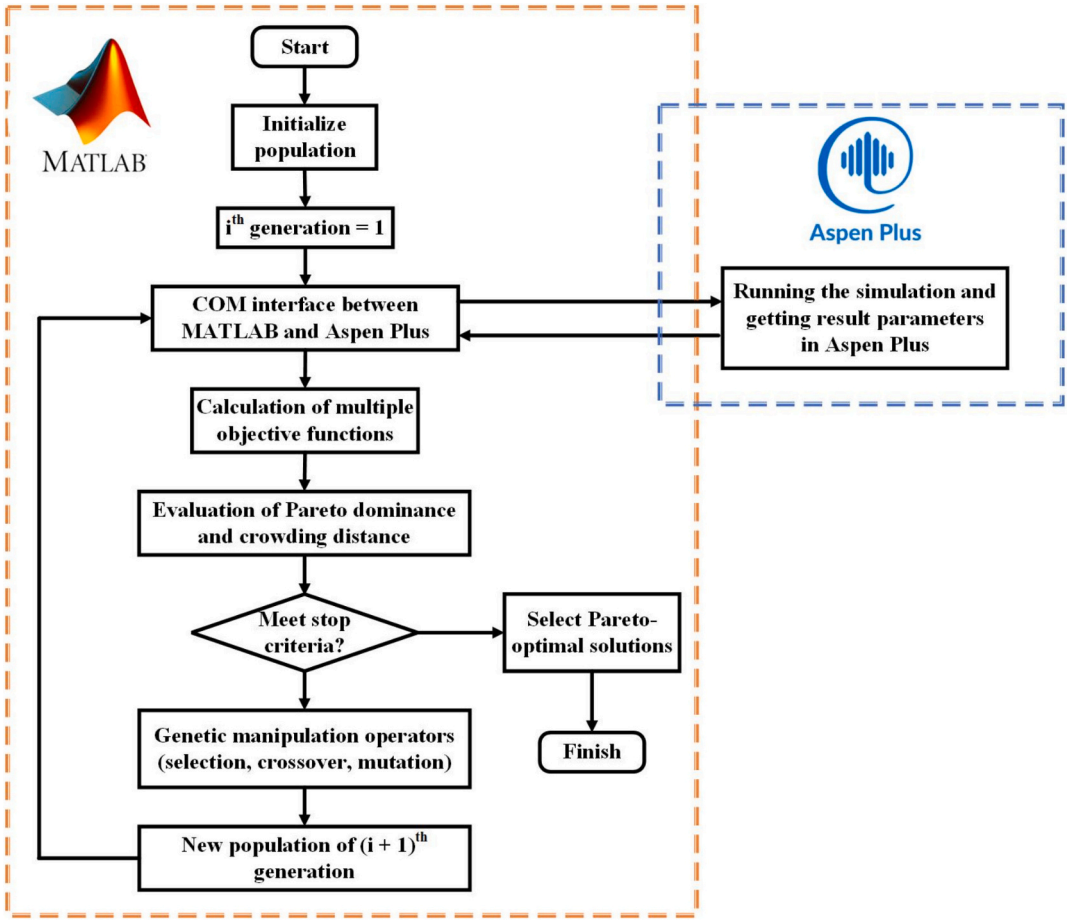

Fig. 5. The MOGA optimization framework of integration of MATLAB and Aspen Plus.

Fig. S2 in the Supporting Information. In terms of the total number of stages, Case 1 requires 36 more stages than Case 2. This is because EG is less effective than GR in enhancing the relative volatility between MeOH and THF. As shown in Fig. 9, the VLE curve for the THF/MeOH mixture with EG as the entrainer is narrower than that with GR, indicating weaker separation capability. Regarding total reboiler duty, Case 2 exhibits a reduction of up to 38.8 % compared to Case 1. Since CO_2 emissions are directly proportional to reboiler duty, this also results in a corresponding environmental benefit. As shown in Eq. 6 and Eq. 7, CO_2 emissions are directly linked to energy consumption in the reboilers. In Case 2, the CO_2 emissions is 437 kg h^{-1}, which is 38.5 % lower than that in Case 1, where the emissions reach 711 kg h^{-1}. This improvement is mainly attributed to the significantly lower entrainer flow rate required in Case 2, which is 67.6 % less (in kmol h^{-1}) than in Case 1. As a result, the REDC bottoms flow rate in Case 2 is 57.9 % lower than in Case 1, while the ERC bottoms flow rate in Case 1 is 64.1 % lower than in Case 2. The lower bottoms flow rates ultimately lead to reduced reboiler duties. These findings support the conclusion that GR is more effective than EG for separating the THF/MeOH mixture, consistent with the report by Raeva and Dubrovsky [67]. One contributing factor is the higher exothermicity of the GD-water reaction compared to the EO-water reaction. Specifically, the GD-water reaction releases 87.8 kJ mol^{-1} of heat [52], whereas the EO-water reaction releases only 80 kJ mol^{-1} [68]. This additional heat release could reduce the reboiler duty, making GD more favorable in the RED configuration.

While Case 1 benefits from a 36.3 % lower total condenser duty compared to Case 2, this advantage does not outweigh its drawbacks. Specifically, Case 1 requires more column stages and has a higher total reboiler duty, both of which contribute to a significantly higher TAC. As shown in the results, Case 1 incurs a TAC of \$ 2.82 $\times$ 10^6 per year, whereas Case 2 achieves a substantially lower TAC of \$ 1.53 $\times$ 10^6 per year or a 45.7 % reduction. It is vital to consider that the TAC of Case 2 already includes the additional costs of a neutralization tank with a volume of 0.025 m^3 and a filter unit with a filtration area of 6.3 m^2. These values were calculated using the equations provided in Table S2 of the Supporting Information. Even with these additional units, Case 2 still offers a better economic outcome than Case 1. Another factor contributing to the superiority of Case 2 is the type of hot utility required. Based on the reboiler temperatures, Case 1 requires low-pressure steam (LPS) for the REDC and high-pressure steam (HPS) for the ERC. In contrast, Case 2 requires only LPS for the REDC and medium-pressure steam (MPS) for the ERC, meaning it can operate with lower-grade (and therefore cheaper) hot utilities. However, Case 2 requires a higher-grade cold utility (i.e., refrigerant water), particularly for the ERC. This is because the optimal pressure for the ERC in Case 2 is 89.5 % lower than in Case 1, resulting in a much lower condenser temperature. The REDC in Case 2 also operates at a lower pressure (up to 23.5 % lower) than in Case 1, although in both cases the condenser temperature remains within the range of standard cooling water.

It is important to note, however, that lower pressure does not always lead to higher vacuum system costs. In this study, the vacuum system cost in Case 2 was observed to be 52.2 % lower than in Case 1, despite operating at lower pressures for both the REDC and ERC. This is because vacuum system cost is influenced not only by pressure but also by column volume (as shown in Table S2 in the Supporting Information). Larger columns incur higher vacuum system costs. The columns in Case 1 have more stages than those in Case 2, leading to larger volumes. Additionally, the REDC diameter in Case 1 is 53.7 % greater than in Case 2. Although the ERC diameter in Case 1 is 9.5 % smaller than in Case 2, this reduction is not sufficient to offset the increased column height and

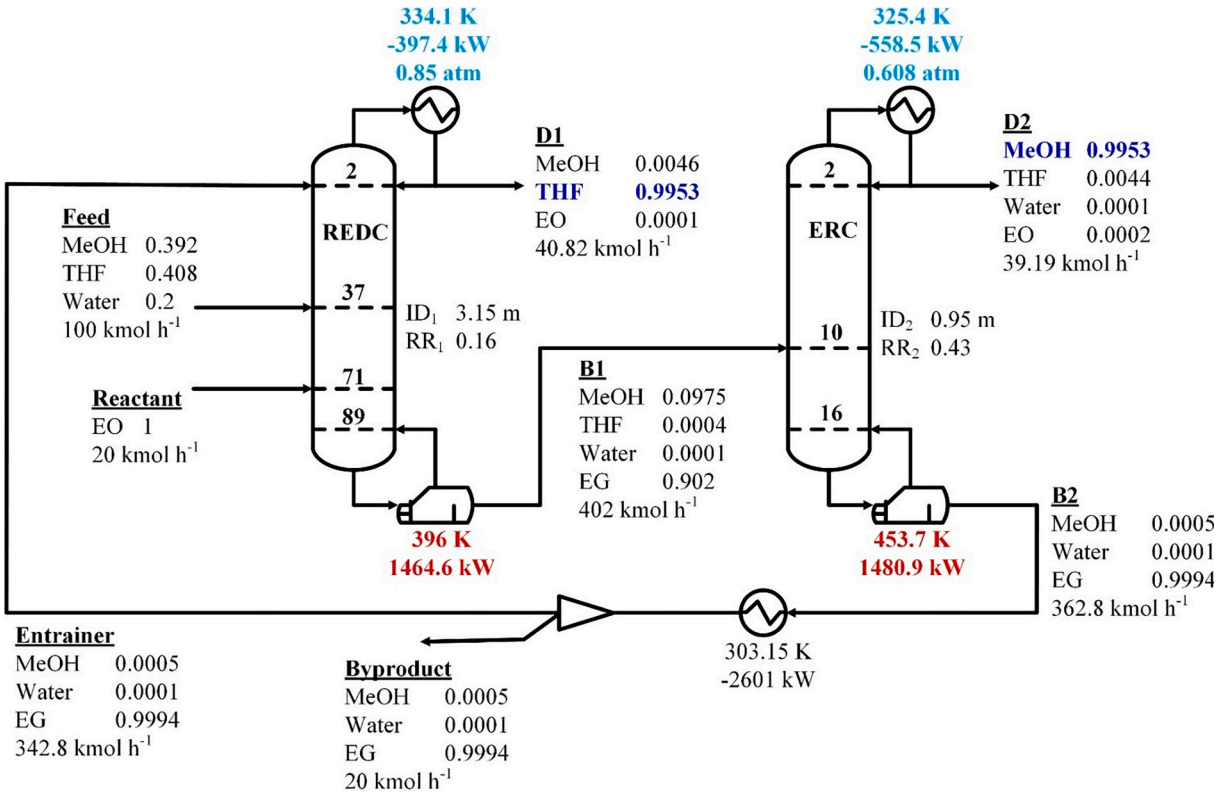

Fig. 6. Optimized flowsheet of Case 1. All compositions are in mole fraction.

thus, does not reduce the overall volume significantly.

Case 1 and Case 2 also differ in terms of reactant and by-product. Case 1 uses EO as the reactant, producing EG as a by-product, while Case 2 uses GD as the reactant, yielding GR. Based on pricing data from Refs. [55,60] (Table S3 in the Supporting Information), GD is 50 % cheaper per kilogram than EO, while GR is 15.8 % more expensive than EG. Combined with the lower TAC, this results in Case 2 achieving a 52 % higher TNR than Case 1. Specifically, Case 1 has a TNR of $\$ 1.79 \times 10^7$ per year, while Case 2 reaches $\$ 2.72 \times 10^7$ per year.

The exergy analysis reveals that exergy destruction in Case 1 is 309 kW, while in Case 2 it is 314.3 kW. However, Case 2 exhibits a slightly higher exergy efficiency of 94.0 %, compared to 92.8 % in Case 1. Although the absolute exergy destruction is marginally higher in Case 2, its efficiency is greater because the proportion of exergy destruction relative to the total input is smaller. Specifically, the exergy input for Case 1 is 4275 kW, whereas for Case 2 it is 5241 kW. From a process design perspective, Case 2 requires more exergy input (up to 22.6 %) and has slightly higher exergy destruction (1.7 %). However, its higher efficiency indicates that the input exergy is converted more effectively into useful work or product. This may be attributed to the nature of the product formed, as Case 2 produces GR, which enhances the separation of THF/MeOH more effectively than EG, the product in Case 1.

3.2. *Surprising finding: Case 3 - SCRED*

Based on the comparison between Case 1 and Case 2, it is evident that Case 2 offers more advantages. The next step was to intensify Case 2 further in the hope of achieving better economic performance, lower environmental impact (in terms of CO_2 emissions), and higher exergy efficiency. The original plan involved applying thermally coupled (ThC) or DW-RED configurations, as these have been widely investigated in the literature [22,31]. These configurations typically require drawing a side stream from the REDC. As shown in Fig. 10, the liquid mole fraction of MeOH in the REDC reaches its maximum at stage 62, with a value of 0.478. Additionally, the vapor mole fraction of MeOH at this stage is already 0.988, making it a logical starting point for placing a side stream. Surprisingly, when a side stream of 39.19 kmol h^{-1} was drawn from this stage, the MeOH mole fraction in this stream already met the target purity ($\geq$ 0.995). A flow rate of 39.19 kmol h^{-1} was selected to match the recovered methanol observed in both Case 1 and Case 2 . This result implies that high-purity THF and MeOH can be recovered using only a single column with THF from the distillate and MeOH from the side stream. Since the design employs just one column, it is referred to as SCRED. It is important to note that some literature reported that ThC-RED and DW-RED have inferior performance than DCRED. For example, Du et al. [19] reported that in the separation of THF/MeOH/water, DW-RED required 4.6 % more reboiler duty than DCRED. Similarly, Teh et al. [31] reported that ThC-RED and DW-RED increased the total reboiler duty by up to 21.5 % and 26.8 %, respectively, compared to DCRED in the separation of an EtAc/EtOH/water mixture. Given these drawbacks, and considering that SCRED has not been previously reported in the context of RED, this study focuses on exploring SCRED as a new configuration.

The optimized SCRED design is shown in Fig. 11. Compared to Case 2, Case 3 exhibits a 31.7 % higher reboiler duty, which is unexpectedly worse. However, as mentioned in previous paragraph, several studies have reported similar trends, where intensified configurations can lead to higher energy consumption or increased TAC [19,31]. Teh et al. [31] speculated that intensified configurations are only beneficial in systems with severe remixing. However, this does not seem to apply in the present work, as severe remixing is also observed in Fig. 10, yet SCRED fails to achieve energy savings. To better understand why SCRED requires a higher reboiler duty, it is necessary to examine the vapor stream leaving the reboiler and returning to the column (the boil-up stream), as the reboiler energy is primarily used to vaporize this stream. The comparison of the boil-up stream of Case 2 and Case 3 is presented in Table 2.

As shown in Table 2, the major component in the boil-up stream of

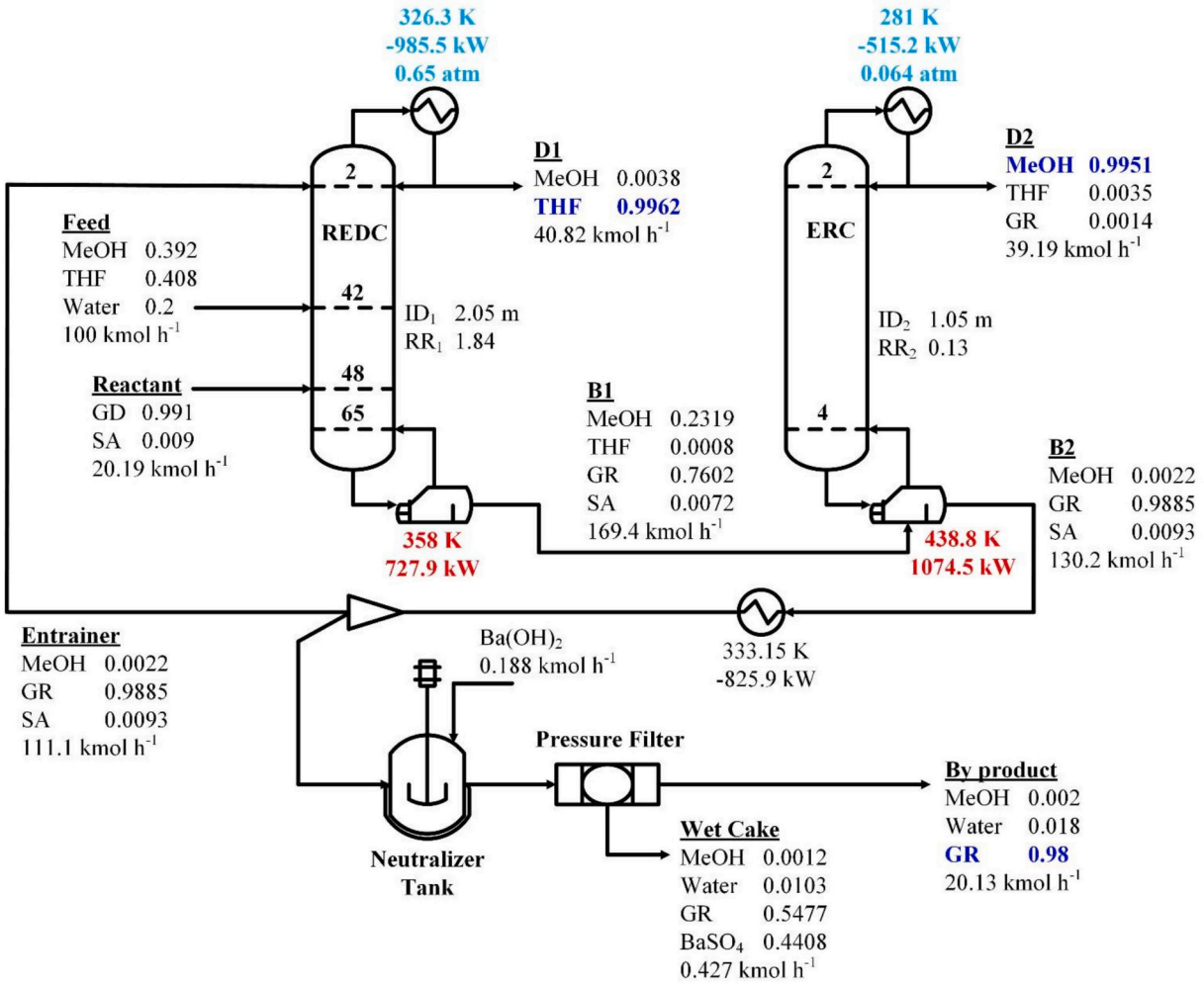

Fig. 7. Optimized flowsheet of Case 2. All compositions are in mole fraction.

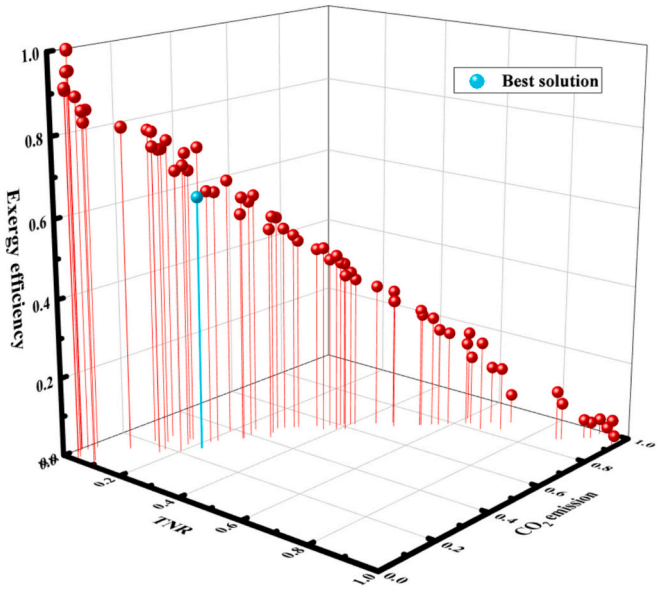

Fig. 8. Final Pareto front for Case 1. Converged after 224 iterations with a total computation time of 120 h. All objective values are normalized to a 0–1 scale.

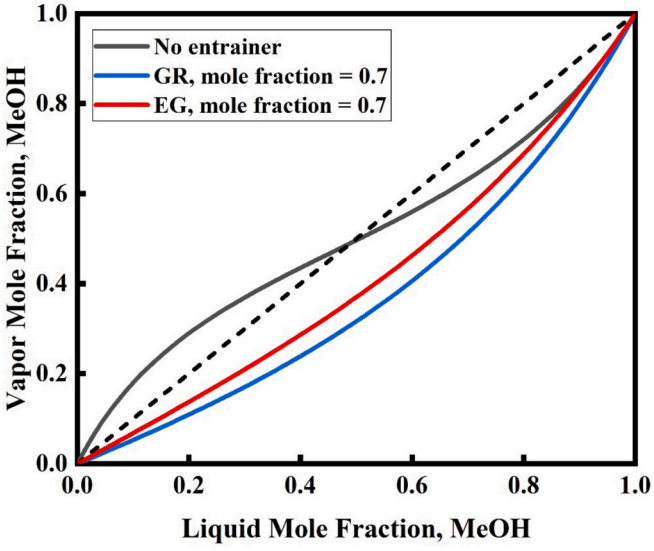

Fig. 9. Entrainer effect on VLE of THF/MeOH at 1 atm.

Case 2 is MeOH, with mole fractions of 0.992 and 0.805 in the REDC and SRC, respectively. In contrast, the boil-up stream in Case 3 is dominated by GR, with a mole fraction of 0.758, as most MeOH has already been

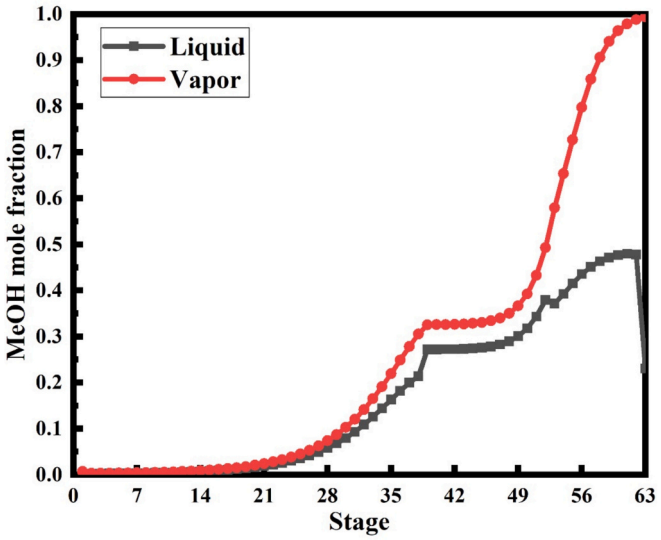

Fig. 10. Profile of MeOH mole fraction in REDC.

withdrawn *via* the side stream. This compositional difference leads to a significant variation in the ΔH_{VL}. According to the Aspen Plus database, pure GR has a ΔH_{VL} that is 156.8 % higher than that of pure MeOH. As a result, a stream rich in GR (as in Case 3) naturally has a higher ΔH_{VL} than one rich in MeOH (as in Case 2). A higher ΔH_{VL} indicates that more energy is required by the reboiler to vaporize the mixture. Although the boil-up flow rate in the REDC of Case 3 is 19.1 % lower than that in Case 2, this reduction is insufficient to offset the effect of the higher ΔH_{VL}. Consequently, the overall reboiler duty in Case 3 becomes higher than in Case 2.

This higher reboiler duty also leads to increased CO_2 emissions and a higher TAC in Case 3 compared to Case 2. CO_2 emissions in Case 3 is 557 kg h^{-1}, which is 27.5 % higher than in Case 2, while the TAC is \$ 1.9 × 10^6 per year, representing a 19.5 % increase over Case 2. This TAC value also already includes the additional costs of a neutralization tank with a volume of 0.025 m^3 and a filter unit with a filtration area of 6.3 m^2. Although Case 3 requires only one column and has eight fewer stages,

Table 2
Boil-up stream comparison between case 2 and case 3.

Parameters	Case 2		Case 3
	REDC	SRC	REDC
Component mole fraction			
MeOH	0.992	0.805	0.234
THF	0.008	0.001	0.001
GR	0	0.193	0.758
SA	0	0.001	0.007
Enthalpy of vaporization (ΔH_{VL}) (kJ $kmol^{-1}$)	34,925	39,457	71,167
Boil-up flow rate (kmol h^{-1})	60.02	13.39	48.56

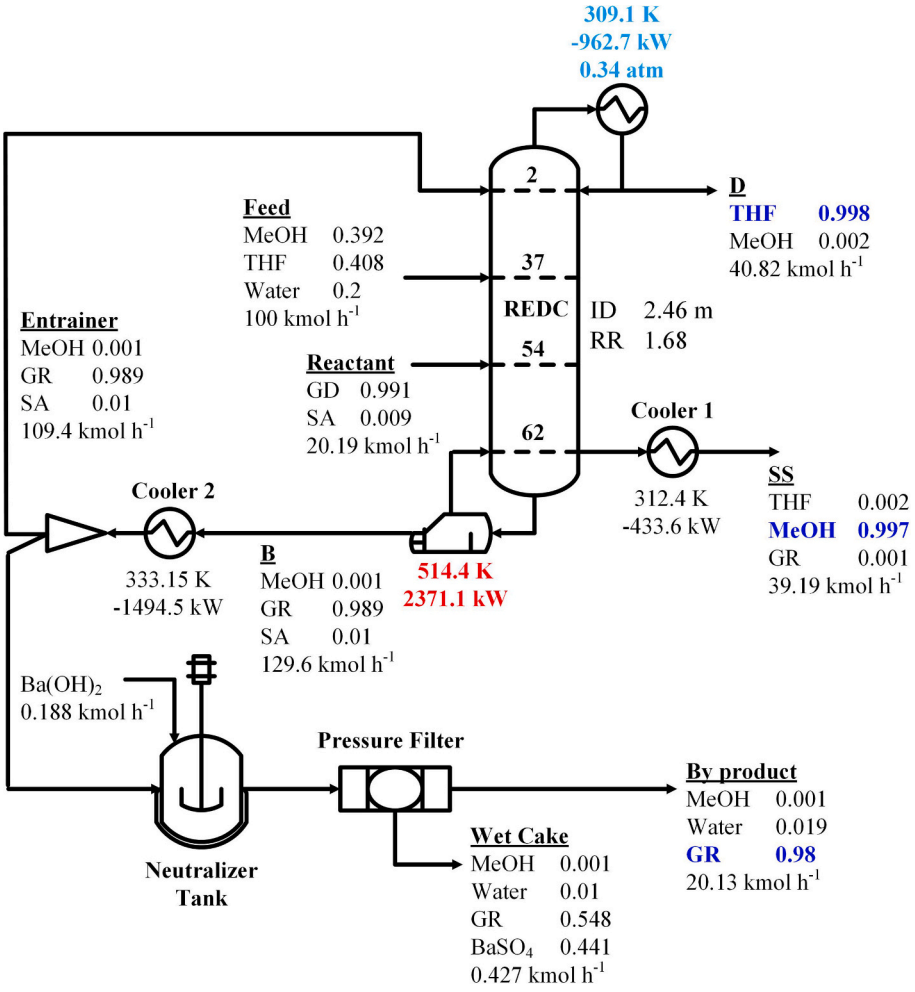

Fig. 11. Optimized flowsheet of Case 3. All compositions are in mole fraction.

the cost savings from these advantages are outweighed by the increased reboiler duty. This can be seen in the economic breakdown where the capital cost in Case 3 is 1.78 % lower than in Case 2, while the operating cost is up to 64.4 % higher. In addition to the total reboiler duty, the significantly higher operating cost is also attributed to the use of hot utilities. While Case 2 uses LPS and MPS, Case 3 requires HPS, which is more expensive. Since the TAC of Case 3 is higher, its TNR is naturally lower than that of Case 2. However, the difference is relatively small, at only 1.1 %, with a TNR of $ 2.69 $\times$ 10^7 per year. This suggests that the gap between the product selling price and the raw material cost (i.e., the terms of $\sum \left(\text{value}_{\text{products}} - \text{cost}_{\text{raw materials}}\right)$ in Eq. 5) has a more significant impact on TNR than the TAC.

In terms of exergy efficiency, Case 3 achieves 93.97 %, which is almost similar to Case 2, with an insignificant difference of only 0.03 %. A breakdown of the exergy shows that the exergy input and exergy destruction in Case 3 are 5242 kW and 315.9 kW, respectively. These values are also very close to those in Case 2. Therefore, overall, Case 3 does not perform better than Case 2, as it provides lower TNR and higher CO_2 emissions, despite having similar exergy efficiency. Although Case 3 does not meet the initial expectations, we hope readers can appreciate the effort made to intensify the DCRED system. Furthermore, as SCRED is introduced for the first time in this study, the result adds to the growing list of intensified RED configurations that do not necessarily improve performance. Similar observations have been reported for ThC-RED and DW-RED in previous studies.

However, compared to Case 1, Case 3 still performs better. It delivers 50.3 % higher TNR and slightly higher exergy efficiency (by 1.17 %). In addition, the reboiler duty and CO_2 emissions are 19.5 % and 21.7 % lower, respectively, than in Case 1. This improvement is mainly due to the significantly higher entrainer flow rate required in Case 1, which leads to increased energy consumption and emissions. These results highlight the suitability of using GR and its associated reaction (i.e., the GD-water reaction) over EG, which is produced from the EO-water reaction. In other words, GD is more suitable than EO as a reactant for separating the THF/MeOH/water mixture using the RED system. Fig. 12 summarizes the 4E metrics for all cases.

4. Conclusion

This study comparatively evaluated three process configurations for separating THF/MeOH/water mixtures *via* RED. Case 1 and Case 2 employed EO and GD as reactants in a DCRED system, respectively, while Case 3 used GD in a SCRED configuration. The results showed that replacing EO with GD improved process sustainability. Although the increase in exergy efficiency was modest (1.2 %), Case 2 achieved significant gains, including 38.5 % lower CO_2 emissions, 38.8 % reductions in total reboiler duty, and 52 % higher TNR relative to Case 1. These improvements are attributed to the formation of GR, which enhances the relative volatility between THF and MeOH. The SCRED configuration, though less efficient than DCRED with GD, still outperformed the EO-based process, confirming that GD is a more effective and sustainable reactant for RED-based separation of THF/MeOH/water mixtures.

The main limitation of this study lies in its scope, which is restricted to simulation work. However, it is important to note that all existing studies on RED for the separation of water-containing ternary mixtures are also based on simulations. Therefore, conducting experimental investigations on RED, as well as thermodynamic model verification by direct experimental data, is a crucial direction for future research. This work also focuses solely on steady-state design. Future studies should consider dynamic analysis and control system development to enhance the practical applicability of the process. In addition, exploring other ternary mixtures is recommended to identify which systems are better suited to EO or GD as the reactant. The development of intensified RED configurations that outperform conventional DCRED systems in terms of

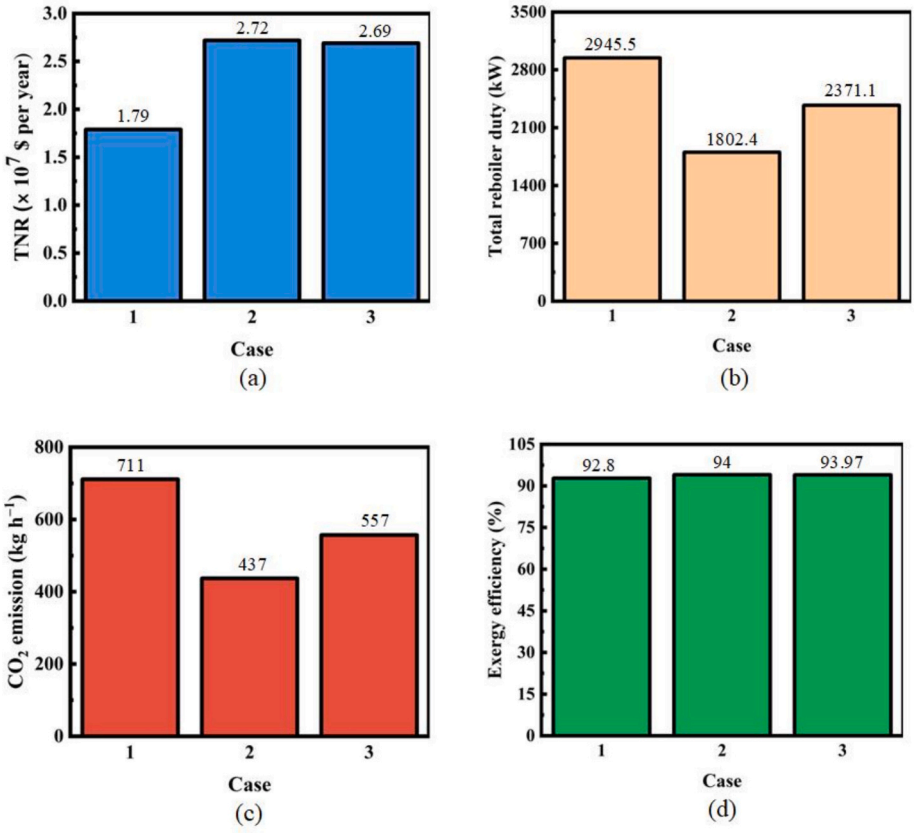

Fig. 12. Comparative performance metrics of Case 1, Case 2, and Case 3: (a) TNR; (b) Total reboiler duty; (c) CO_2 emissions; and (d) Exergy efficiency.

energy efficiency and economic performance is another promising area for future work. Finally, in-depth investigation of optimization methods is recommended. This includes comparing various optimization approaches and examining the influence of optimization parameters on both the optimization process and its outcomes.

CRediT authorship contribution statement

I Gede Pandega Wiratama: Writing – original draft, Data curation, Conceptualization. **Zong Yang Kong:** Writing – review & editing, Supervision, Project administration, Investigation, Conceptualization. **Ao Yang:** Writing – review & editing, Investigation, Conceptualization. **Agus Saptoro:** Writing – review & editing, Supervision, Resources, Formal analysis. **Basil T. Wong:** Resources. **Juan Gabriel Segovia-Hernández:** Writing – review & editing, Resources. **Jaka Sunarso:** Writing – review & editing, Supervision, Resources, Project administration, Formal analysis.

Declaration of competing interest

Dr. Zong Yang Kong also serves as an Editorial Board Member (Early Career) for Separation and Purification Technology at the time of manuscript submission.

Acknowledgments

I Gede Pandega Wiratama would like to acknowledge the support from Swinburne University of Technology Sarawak Campus in the form of Full Fee-Waiver Studentship for his Doctor of Philosophy.

Appendix A. Supplementary data

Supplementary data to this article can be found online at https://doi.org/10.1016/j.seppur.2025.136001.

Data availability

Data will be made available on request.

References

[1] Y. Su, A. Yang, S. Jin, W. Shen, P. Cui, J. Ren, Investigation on ternary system tetrahydrofuran/ethanol/water with three azeotropes separation via the combination of reactive and extractive distillation, J. Clean. Prod. 273 (2020) 123145, https://doi.org/10.1016/j.jclepro.2020.123145.

[2] C. Wang, Y. Zhuang, L. Liu, L. Zhang, J. Du, Design and comparison of energy-saving double column and triple column reactive-extractive hybrid distillation processes for ternary multi-azeotrope dehydration, Sep. Purif. Technol. 259 (2021) 118211, https://doi.org/10.1016/j.seppur.2020.118211.

[3] Y. Wang, W. Zhu, H. Cheng, J. Zhong, X. Li, J. Qi, et al., Enhanced reaction extraction distillation via multi-objective optimization and 4E analysis for sustainable recovery of organic compounds from wastewater, Process. Saf. Environ. Prot. 186 (2024) 884–894, https://doi.org/10.1016/j.psep.2024.04.064.

[4] J. Liu, J. Yan, W. Liu, J. Kong, Y. Wu, X. Li, et al., Design and multi-objective optimization of reactive-extractive dividing wall column with organic Rankine cycles considering safety, Sep. Purif. Technol. 287 (2022) 120512, https://doi.org/10.1016/j.seppur.2022.120512.

[5] Z.Y. Kong, G.C. Zarazúa, H.-Y. Lee, J. Chua, J.G. Segovia-Hernández, J. Sunarso, Design of novel side-stream hybrid reactive-extractive distillation for sustainable ternary separation of THF/ethanol/water using mixed entrainer, Process. Saf. Environ. Prot. 166 (2022) 574–588, https://doi.org/10.1016/j.psep.2022.08.056.

[6] Z.Y. Kong, E. Sánchez-Ramírez, A. Yang, W. Shen, J.G. Segovia-Hernández, J. Sunarso, Process intensification from conventional to advanced distillations: past, present, and future, Chem. Eng. Res. Des. 188 (2022) 378–392, https://doi.org/10.1016/j.cherd.2022.09.056.

[7] I.G.P. Wiratama, Z.Y. Kong, A. Yang, A. Saptoro, B.T. Wong, J. Zheng, et al., A quest to find a new reactant to replace ethylene oxide in reactive-extractive distillation for ternary azeotropic separation, Ind. Eng. Chem. Res. 64 (6) (2025) 2369–2381, https://doi.org/10.1021/acs.iecr.4c04602.

[8] Sigma-Aldrich, Ethylene Oxide Safety Data Sheet. https://www.sigmaaldrich.com/ID/de/sds/aldrich/387614?userType=undefined (accessed June 5, 2024).

[9] FSCIMAGE, Material Safety Data Sheet Glycidol. https://fscimage.fishersci.com/msds/93805.htm (accessed October 30, 2024).

[10] Inchem, Glycidol Safety Data Sheet. https://www.inchem.org/documents/icsc/icsc/eics0159.htm#:~:text=Flash%20point%3A%2072%C2%B0C%20c.c (accessed June 5, 2024).

[11] I.G.P. Wiratama, Z.Y. Kong, A. Yang, A. Saptoro, B.T. Wong, J. Zheng, et al., A comprehensive review of reactive-extractive distillation (RED) for production and recovery applications, Ind. Eng. Chem. Res. 64 (26) (2025) 12881–12907, https://doi.org/10.1021/acs.iecr.5c00782.

[12] Y. Li, T. Sun, Q. Ye, J. Li, Y. Xu, X. Jian, Economic and environmental assessment for purification of acetonitrile and isopropanol by reactive coupling extractive distillation, Sep. Purif. Technol. 275 (2021) 119133, https://doi.org/10.1016/j.seppur.2021.119133.

[13] Y.-R. Zhang, T.-W. Wu, I.L. Chien, Intensified hybrid reactive-extractive distillation process for the separation of water-containing ternary mixtures, Sep. Purif. Technol. 279 (2021) 119712, https://doi.org/10.1016/j.seppur.2021.119712.

[14] Z.Y. Kong, A. Yang, J. Chua, J.J. Chew, J. Sunarso, Energy-efficient hybrid reactive-extractive distillation with a preconcentration column for recovering isopropyl alcohol and diisopropyl ether from wastewater: process design, optimization, and intensification, Ind. Eng. Chem. Res. 61 (30) (2022) 11156–11167, https://doi.org/10.1021/acs.iecr.2c01768.

[15] T.-W. Wu, I.L. Chien, Novel control strategy of intensified hybrid reactive-extractive distillation process for the separation of water-containing ternary mixtures, Sep. Purif. Technol. 294 (2022) 121159, https://doi.org/10.1016/j.seppur.2022.121159.

[16] T.-W. Wu, H.-C. Hua, C.-T. Kuo, I.L. Chien, Novel process development of hybrid reactive-extractive distillation system for the separation of a cyclohexane/isopropanol/water mixture with different feed compositions, Ind. Eng. Chem. Res. 62 (5) (2022) 2080–2089, https://doi.org/10.1021/acs.iecr.2c02889.

[17] J. Yan, J. Liu, J. Ren, Y. Wu, X. Li, T. Sun, et al., Design and multi-objective optimization of hybrid reactive-extractive distillation process for separating wastewater containing benzene and isopropanol, Sep. Purif. Technol. 290 (2022) 120915, https://doi.org/10.1016/j.seppur.2022.120915.

[18] A. Yang, Y. Su, S. Sun, W. Shen, M. Bai, J. Ren, Towards sustainable separation of the ternary azeotropic mixture based on the intensified reactive-extractive distillation configurations and multi-objective particle swarm optimization, J. Clean. Prod. 332 (2022) 130116, https://doi.org/10.1016/j.jclepro.2021.130116.

[19] L. Du, S. Jin, Z. Yang, S. Sun, A. Yang, W. Shen, An efficient multi-criteria decision making for assessing the optimization of reactive extractive distillation in terms of economy, environment and safety, Chem. Eng. Res. Des. 197 (2023) 838–850, https://doi.org/10.1016/j.cherd.2023.08.033.

[20] J. Huang, Q. Zhang, C. Liu, T. Yin, W. Xiang, Optimal design of the ternary azeotrope separation process assisted by reactive-extractive distillation for ethyl acetate/isopropanol/water, Sep. Purif. Technol. 306 (2023) 122708, https://doi.org/10.1016/j.seppur.2022.122708.

[21] Z.Y. Kong, A. Yang, C.-C. Tsai, V.S.K. Adi, A. Saptoro, J. Sunarso, Design and optimization of hybrid reactive-extractive distillation for ternary azeotropic separation: a case considering the effect of side reactions, Ind. Eng. Chem. Res. 62 (27) (2023) 10601–10610, https://doi.org/10.1021/acs.iecr.3c01532.

[22] J. Liu, G. Wan, M. Dong, J. Kong, Y. Wu, S. Han, et al., Dynamic controllability strategy of reactive-extractive dividing wall column for the separation of water-containing ternary azeotropic mixture, Sep. Purif. Technol. 304 (2023) 122338, https://doi.org/10.1016/j.seppur.2022.122338.

[23] A. Yang, Z.Y. Kong, J. Sunarso, Design and optimisation of novel hybrid side-stream reactive-extractive distillation for recovery of isopropyl alcohol and ethyl acetate from wastewater, Chem. Eng. J. 451 (2023) 138563, https://doi.org/10.1016/j.cej.2022.138563.

[24] Y.-Y. Chen, Z.Y. Kong, H.-Y. Lee, A new hybrid reactive-extractive distillation configuration for ternary azeotropic separation with intensification opportunity, Sep. Purif. Technol. 335 (2024) 126220, https://doi.org/10.1016/j.seppur.2023.126220.

[25] J. Huang, Y. Chen, Q. Zhang, C. Liu, T. Yin, W. Xiang, Dynamic control strategy of the ternary azeotrope separation process assisted by reactive-extractive distillation for ethyl acetate/isopropanol/water, Chem. Eng. Process. Process Intensif. 199 (2024) 109762, https://doi.org/10.1016/j.cep.2024.109762.

[26] F. Neyestani, R. Eslamloueyan, A novel reactive-extractive distillation process for separation of water/methanol/tetrahydrofuran mixtures, Sci. Rep. 14 (1) (2024) 1931, https://doi.org/10.1038/s41598-024-52427-3.

[27] L. Qi, S. Sun, F. Cheng, A. Aqsha, Z.Y. Kong, J. Sunarso, Exploration of different water content on the performance of reactive-extractive distillation for separating the ternary azeotropic mixture, Sep. Purif. Technol. 334 (2024) 125785, https://doi.org/10.1016/j.seppur.2023.125785.

[28] Q. Rui, Q. Ye, J. Li, Y. Wang, A. Yu, Design and multi-objective optimization of novel side-stream reactive-extractive distillation process with intermediate reboiler for recovering ethanol and 1,4-dioxane from wastewater, Sep. Purif. Technol. 334 (2024) 126127, https://doi.org/10.1016/j.seppur.2023.126127.

[29] E. Sánchez-Ramírez, S. Sun, J.Y. Sim, A. Yang, Z.Y. Kong, J.G. Segovia-Hernández, A more appropriate way to optimize the hybrid reactive-extractive distillation system, Sep. Purif. Technol. 344 (2024) 127184, https://doi.org/10.1016/j.seppur.2024.127184.

[30] I.A.X. Teh, Z.Y. Kong, A. Yang, A. Aqsha, J. Sunarso, Exploring the impact of side-reactions on triple-column reactive-extractive distillation, J. Chem. Technol. Biotechnol. 99 (7) (2024) 1493–1503, https://doi.org/10.1002/jctb.7658.

[31] I.A.X. Teh, H.-Y. Lee, Z.Y. Kong, A. Putranto, J. Zheng, J. Sunarso, Unfavorable process intensification of double column reactive extractive distillation system, Chem. Eng. Process. Process Intensif. 196 (2024) 109657, https://doi.org/10.1016/j.cep.2023.109657.

[32] T. Yin, Q. Zhang, Y. Chen, C. Liu, W. Xiang, Process design and optimization of the reactive-extractive distillation process assisted with reaction heat recovery via side vapor recompression for the separation of water-containing ternary azeotropic mixture, Process. Saf. Environ. Prot. 184 (2024) 1041–1056, https://doi.org/10.1016/j.psep.2024.02.045.
[33] F. Zhang, Z. Li, B. Shan, Z. Zhu, Y. Wang, Q. Xu, Economical process design of reactive-extractive distillation combining variable pressure and heat integration for separating a ternary azeotropic mixture, Energy 312 (2024) 133562, https://doi.org/10.1016/j.energy.2024.133562.
[34] Z.Y. Kong, E. Sánchez-Ramírez, A. Yang, Y. Li, J.G. Segovia-Hernández, B.T. Wong, et al., A new alternative route for achieving energy saving in intensified reactive-extractive distillation system with a surprise discovery, Chem. Eng. J. 503 (2025) 158498, https://doi.org/10.1016/j.cej.2024.158498.
[35] C. Liu, A. Karagoz, O. Alqusair, Y. Ma, X. Xiao, J. Li, Design of hybrid reactive-extractive distillation for separation of azeotropic ternary mixture using a systematic optimization framework, Sep. Purif. Technol. 369 (2025) 132805, https://doi.org/10.1016/j.seppur.2025.132805.
[36] Y. Zhu, H. Chen, N. Li, Y. Liu, R. Wang, Reactive-extractive distillation processes design for aqueous ternary azeotrope separation, Appl. Therm. Eng. 274 (2025) 126703, https://doi.org/10.1016/j.applthermaleng.2025.126703.
[37] A. Zou, G. Zhang, S. Sun, J. Sunarso, L. Qi, Insight into the rational design of reactive-extractive distillation for separating water/toluene/n-butanol via an improved sequential iterative optimisation, Sep. Purif. Technol. 365 (2025) 132669, https://doi.org/10.1016/j.seppur.2025.132669.
[38] Z. Jin, H. Liu, Z. Dai, M. Gao, Y. Dai, Inherent safety evaluation and optimization for the separating tetrahydrofuran/methanol/water ternary system, Sep. Purif. Technol. 377 (2025) 134503, https://doi.org/10.1016/j.seppur.2025.134503.
[39] D.S. Sholl, R.P. Lively, Seven chemical separations to change the world, Nature 532 (7600) (2016) 435–437, https://doi.org/10.1038/532435a.
[40] J. Rogelj, M. Den Elzen, N. Höhne, T. Fransen, H. Fekete, H. Winkler, et al., Paris agreement climate proposals need a boost to keep warming well below 2 °c, Nature 534 (7609) (2016) 631–639, https://doi.org/10.1038/nature18307.
[41] H. Alcocer-García, J.G. Segovia-Hernández, O.A. Prado-Rubio, E. Sánchez-Ramírez, J.J. Quiroz-Ramírez, Multi-objective optimization of intensified processes for the purification of levulinic acid involving economic and environmental objectives, Chem. Eng. Process. Process Intensif. 136 (2019) 123–137, https://doi.org/10.1016/j.cep.2019.01.008.
[42] Q. Zhao, X. Chu, Y. Li, M. Yan, X. Wang, Z. Zhu, et al., Economic, environmental, exergy (3E) analysis and multi-objective genetic algorithm optimization of isopropyl acetate production with hybrid reactive-extractive distillation, Sep. Purif. Technol. 301 (2022) 121973, https://doi.org/10.1016/j.seppur.2022.121973.
[43] Z. Jin, H. Liu, Z. Dai, Y. Dai, Investigation on energy-saving distillation for separating tetrahydrofuran/methanol/water ternary azeotropic system, J. Clean. Prod. 441 (2024) 140899, https://doi.org/10.1016/j.jclepro.2024.140899.
[44] J. Gu, X. You, C. Tao, J. Li, V. Gerbaud, Energy-saving reduced-pressure extractive distillation with heat integration for separating the biazeotropic ternary mixture tetrahydrofuran–methanol–water, Ind. Eng. Chem. Res. 57 (40) (2018) 13498–13510, https://doi.org/10.1021/acs.iecr.8b03123.
[45] Z.A. Antonova, V.S. Kruk, V.N. Kursevich, Y.V. Maksimuk, V.D. Sokolov, On separating mixtures containing methanol, tetrahydrofuran, and water by distillation, Russ. J. Appl. Chem. 85 (9) (2012) 1447–1453, https://doi.org/10.1134/s1070427212090248.
[46] X. Liu, Q. Xu, C. Ma, F. Zhang, P. Cui, Y. Wang, et al., Design and multi-objective optimization of reactive pressure-swing distillation process for separating tetrahydrofuran-methanol-water, Sep. Purif. Technol. 329 (2024) 125160, https://doi.org/10.1016/j.seppur.2023.125160.
[47] C. Yang, S. Ma, X. Yin, Organic salt effect of tetramethylammonium bicarbonate on the vapor–liquid equilibrium of the methanol–water system, J. Chem. Eng. Data 56 (10) (2011) 3747–3751, https://doi.org/10.1021/je200341c.
[48] Q. Li, P. Liu, L. Cao, F. Wen, S. Zhang, B. Wang, Vapor–liquid equilibrium for tetrahydrofuran+methanol+tetrafluoroborate-based ionic liquids at 101.3kPa, Fluid Phase Equilib. 360 (2013) 439–444, https://doi.org/10.1016/j.fluid.2013.09.060.
[49] S.M. Danov, A.V. Sulimov, A.V. Ovcharova, Vapor-liquid equilibria in the system of glycidol synthesis products, Theor. Found. Chem. Eng. 47 (5) (2013) 563–569, https://doi.org/10.1134/S0040579513040192.
[50] K. Huang, M. Nakaiwa, S.-J. Wang, A. Tsutsumi, Reactive distillation design with considerations of heats of reaction, AICHE J. 52 (7) (2006) 2518–2534, https://doi.org/10.1002/aic.10885.
[51] Z.Y. Kong, J. Sunarso, A. Yang, Recent progress on hybrid reactive-extractive distillation for azeotropic separation: a short review, Front. Chem. Eng. 4 (2022) 1–6, https://doi.org/10.3389/fceng.2022.986411.
[52] D.P. Vermeulen, J.M.H. Fortuin, A.G. Swenker, Experimental verification of a model describing large temperature oscillations of a limit-cycle approaching liquid-phase reaction system in a CSTR, Chem. Eng. Sci. 41 (5) (1986) 1291–1302, https://doi.org/10.1016/0009-2509(86)87102-0.
[53] A.A. Kiss, Novel catalytic reactive distillation processes for a sustainable chemical industry, Top. Catal. 62 (2018), https://doi.org/10.1007/s11244-018-1052-9 (17-20) 1132-48.
[54] W.L. Luyben, C.-C. Yu, Reactive Distillation Design and Control, John Wiley & Sons, Inc., Hoboken, 2008.
[55] Made-in-China.com. https://www.made-in-china.com/ (accessed March 17, 2025).
[56] M.L. Donten, J. Vandevondele, P. Hamm, Speed limits for acid-base chemistry in aqueous solutions, Chimia (Aarau) 66 (4) (2012) 182–186, https://doi.org/10.2533/chimia.2012.182.
[57] Transforming starch processes with automatic pressure filters, in: MetsoAutotec (Ed.), MetsoAutotec, Metso Autotec, 2020.
[58] J.M. Douglas, Conceptual Design of Chemical Processes, McGraw-Hill, New York, 1988.
[59] D.E. Garrett, Chemical Engineering Economics, Van Nostrand Reinhold, New York, 1989.
[60] Chemical-Book.com. https://www.chemicalbook.com/ (accessed September 1, 2024).
[61] B. Dai, H. Qi, S. Liu, Z. Zhong, H. Li, M. Song, et al., Environmental and economical analyses of transcritical CO_2 heat pump combined with direct dedicated mechanical subcooling (DMS) for space heating in China, Energy Convers. Manag. 198 (2019) 111317, https://doi.org/10.1016/j.enconman.2019.01.119.
[62] J.D. Seader, E.J. Henley, D.K. Roper, Separation Process Principles, Wiley, New York, 1998.
[63] J. Szargut, Chemical exergies of the elements, Appl. Energy 32 (4) (1989) 269–286, https://doi.org/10.1016/0306-2619(89)90016-0.
[64] M. Abudoureheman, Y. Shi, B. Wei, Y. Zhao, Energy efficiency analysis and optimization of heat exchange network under the goal of “double carbon”: a case for production process of isopropyl acetate, Energy Sourc. Part A: Recov. Utilizat. Environ. Eff. 46 (1) (2024) 2080–2092, https://doi.org/10.1080/15567036.2024.2302380.
[65] H.S. Eldarsi, P.L. Douglas, Methyl-tert-butyl-ether catalytic distillation column, Chem. Eng. Res. Des. 76 (4) (1998) 517–524, https://doi.org/10.1205/026387698524992.
[66] C. Wang, T. Sun, W. Chen, Z. Tan, Y. Zhuang, J. Du, et al., Applicability exploration and sustainable assessment of heat integration and vapor recompression heat pump to side-stream extractive distillation processes for separating ternary azeotropic system, Sep. Purif. Technol. 345 (2024) 127251, https://doi.org/10.1016/j.seppur.2024.127251.
[67] V.M. Raeva, A.M. Dubrovsky, Comparison of extractive distillation flowsheets for methanol–tetrahydrofuran–water mixtures, Fine Chem. Technol. 15 (3) (2020) 21–30, https://doi.org/10.32362/2410-6593-2020-15-3-21-30.
[68] Y. Tavan, R.M. Behbahani, S.H. Hosseini, A novel intensified reactive distillation process to produce pure ethyl acetate in one column—part I: parametric study, Chem. Eng. Process. Process Intensif. 73 (2013) 81–86, https://doi.org/10.1016/j.cep.2013.05.015.